Malaysian Journal of Mathematical Sciences 17(4): 531–556 (2023)
https://doi.org/10.47836/mjms.17.4.02

Malaysian Journal of Mathematical Sciences

Journal homepage: https://mjms.upm.edu.my

Pricing Quanto Options in Renewable Energy Markets

Arsat, N. A. A.[1], Ibrahim, N. A.*[1], and Taib, C. M. I. C.[2]

[1]*Faculty of Science and Technology, Islamic Science University of Malaysia, Bandar Baru Nilai, 71800, Nilai, Negeri Sembilan, Malaysia*
[2]*Faculty of Ocean Engineering Technology and Informatics, University Malaysia Terengganu, 21030 Kuala Nerus, Terengganu, Malaysia*

E-mail: nooradilah@usim.edu.my
**Corresponding author*

Received: 18 July 2023
Accepted: 20 October 2023

Abstract

High level of greenhouse gases emission in fossil fuels has induced a significant transition from conventional energy sources to renewable energy. However, using renewable energy in electricity grids has limitations, such as intermittency and lack of efficient energy storage. This paper focuses on constructing the quanto options contract to help renewable energy producers hedge the risk against low photovoltaic (PV) production and electricity prices. To achieve our objective, we first model the interday PV power production with a combination of a deterministic and stochastic model. We analyse empirical data for daily solar production in three operators in Germany ranging from 1 January 2016 to 31 December 2020. We discovered that all estimated parameters of the deterministic process are highly significant. Meanwhile, we use an autoregressive (AR) process to describe the random behavior in the production. The results demonstrated that AR(2) is suitable enough to explain its stochastic factor. For the error terms analysis, we observed a clear sign of seasonal heteroskedasticity supported by the left skewed density. In addition, we observed a clear seasonal pattern in the squared error terms, where we suggest using seasonal variance and skewed normal distribution to describe its dynamic. As for an application, we embed the PV model in the power price modeling. We found that AR(3) process is sufficient to explain the price behavior and that normal distribution best fits the error terms. Using the suggested PV and power price model, we construct the quanto options contract for renewable energy producers using Monte Carlo simulations. We discovered that the electricity price payoffs are consistent throughout the year, whereas PV and quanto options payoffs vary greatly depending on the season. The quanto options price result shows that the prices vary during four seasons, with the highest variation in July.

Keywords: photovoltaic productions; electricity prices; Quanto options.

1 INTRODUCTION

In the contemporary age, the world's electricity consumption has increased, which induced high utilization of fossil fuels such as coal, oil, and gas. Extreme consumption of fossil fuels may emit a high level of greenhouse gases such as carbon dioxide, methane, and nitrous oxide [19]. Figure 1 shows the overview of U.S. greenhouse gases emission in 2020. These gases may increase not only the global temperature but also threaten the health of human beings. This issue is becoming a debatable topic around the world on how to overcome this problem. Climate change and local air pollution are the most significant global energy transition issues. For example, air pollution is a primary driver in countries like China and India [21]. However, the adverse health impacts of air pollution, mainly related to energy supply and usage, are also gaining attention in European countries. To overcome this genuine issue, most countries worldwide are transforming their non-renewable energy sources to renewable energies, such as PV, wind, biomass, and geothermal, which are much cleaner, safer, and cheaper. This transformation also may reduce the cost of universal energy access, enhance health, boost energy safety, and diversify energy supplies.

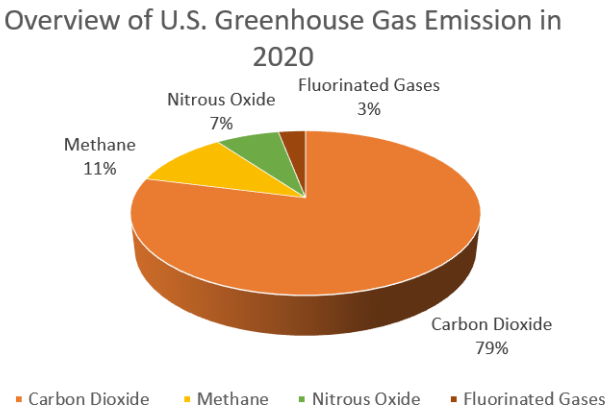

Figure 1: Overview of U.S. Greenhouse Gases Emission in 2020. (Source: Inventory of U.S. Greenhouse Gas Emissions and Sinks: 1990 - 2020).

The announcement of the Sustainable Development Goals (SDGs) by the United Nations General Assembly (UNGA) has created a practical framework for global cooperation to create a sustainable future for the earth [21]. One of the 17 lists of SDGs focuses on the production of affordable and clean energy. In contrast to all types of renewable energy, solar power is becoming one of the fastest developed in the world energy sources. It is now the second place for renewable energy technology, after wind, in terms of installed capacity [26]. Despite the tremendous increase in demand in recent years, the cost of solar PV modules and inverters has decreased, rewarding project developers but harming manufacturers who have battled to maintain profits.

However, renewable energy has its limitations. The most critical factors are intermittent sources and insufficient storage for excess energy production. For instance, PV power can only be produced during the day with the presence of the sun, and there will be no production at night. Since there is no efficient storage to store the energy produced, it must be consumed once produced. Furthermore, forecasting the amount of solar radiation that a photovoltaic panel will capture is a complex task due to the influence of cloudiness and fluctuations in solar irradiance.Voluminous studies have discussed the efficiency of PV panels to maximize production [13, 27]. However, there are limited references studied on financial perspectives. Since the sun intensity and cloud

cover are the essential factors in determining the amount of PV generation, we forecast the PV production by considering both the deterministic and stochastic factors represented by the sun intensity and cloud cover, respectively.

The literature on stochastic models for electricity pricing and different commodities has increased rapidly in previous years. Many researchers have discovered that the models commonly utilized in financial markets are irrelevant because of the unique features of commodity prices, especially electricity prices. Dutta and Mitra [18] have discussed the literature on various topics related to dynamic electricity pricing and recorded future research possibilities related to pricing policy, consumer eagerness to pay, and market segmentation in this area. Furthermore, Borovkova and Schmeck [11] and Deng et al. [16] uses the Monte Carlo simulation to explain the electricity price, while Biagini et al. [10] simplify modeling an electricity futures market with a risky asset added.

As aforementioned, intermittency is the foremost hurdle to using renewable energy. PV power can only be generated in the presence of the sun. This results in no production at night which can be overcome with fossil fuels generation. A low volume of PV production may lead to high production of non-renewable. This may lead to low electricity prices if the supply exceeds demand. As a result, renewable energy producers will be hit twice due to low energy production (renewable energy) and low power price. To overcome such risk, renewable energy producers can enter a derivative contract to hedge their risk exposure, such as a quanto options derivatives contract.

There are many past studies researched on weather derivatives contracts. For example, Esunge and Njong [20], Tastan and Hayfavi [34] and Wang et al. [37] had been introduced to cover the risk exposure from weather conditions with different approaches such as the Ornstein-Uhlenbeck process and Monte Carlo simulations. In addition, Cui and Anatoliy [14] also conducted a study analyzing various types of weather-related risks in different industries. They proposed a dynamic hedging strategy to hedge time-ahead energy using temperature futures. Nevertheless, there are minimal sources of quanto options derivatives, especially in the energy market. The quanto options typically refer to derivatives used to hedge foreign exchange fee risk, wherein the asset is denominated with one currency but resolved in another. There are few past research related to the pricing of currency quanto options [30, 35], which derive and develop a strategy for pricing the quanto option. In energy markets, Benth et al. [4] evolved a quanto options rate concerning wind energy production and electricity price, while Benth et al. [6] have derived analytical solutions of quanto options rate on futures contracts and a temperature index. In this study, we are keen to investigate if quanto options may help renewable energy producers to mitigate their volume and price risk simultaneously.

Generally, there are two types of models to forecast the production of PV such as parametric and non-parametric. The parametric model (deterministic or physical) summarizes meteorological factors such as sun irradiation and temperature on solar cells. On the other hand, the non-parametric (stochastic) model does not assume any knowledge of the internal system. It is noteworthy to mention that many studies that applied a non-parametric technique had been successfully conducted by including machine learning models, Support Vector Machine (SVM) [38, 31], Numerical Weather Prediction (NWP) [1, 29] and some improvement on Artificial Neural Network (ANN) [39, 17, 32]. Unfortunately, both parametric and non-parametric have their pros and cons. The parametric model, for example, necessitates a few variables, such as ambient and cell conditions. On the other hand, non-parametric models are frequently chastised for lacking historical data, being computationally complicated, and having a significant possibility of overfitting. Moreover, since solar energy is nonlinear and fluctuates, thus a single forecasting model is insufficient to represent real generation behavior [39]. By proposing a simpler model which is powerful enough to represent the concept of forecasting PV generation, this hybrid model is

expected to contribute more. For example, Benth and Ibrahim [5] proposed a simple model but sophisticated enough to forecast PV production. We use that proposed model since it captured the seasonality behavior of the data very well using a discrete-time AR process. For our study, we want to investigate further if the continuous-time AR process may contribute to modeling the PV and power prices. This is an essential step before pricing the quanto options, where pricing the derivatives requires a continuous-time process.

In this study, we concentrate on estimating the PV production in three German transmission system operators: 50Hertz, Amprion, and TransnetBW. An empirical analysis of German photovoltaic (PV) production is conducted in Section 2. This analysis involves examining the trend and seasonal component, utilizing a continuous autoregressive (CAR) process to model the stochastic behavior, and fitting the residuals with a suitable distribution. In the subsequent section, we model the simulated power sot prices using the proposed photovoltaic (PV) production model as discussed in previous section. Section 4 of this paper presents an analysis of an application to PV based options namely quanto option followed by the conclusion.

2 PV Power Generation Analysis

2.1 Data description

In this section, we describe the PV production data. The data are obtained from German operators. The photovoltaic (PV) data was gathered over a period spanning from January 1st, 2016 to December 31st, 2020. All of the data were retrieved from their general websites; https://www.50hertz.com/en/, https://www.amprion.net/index-2.html and https://www.transnetbw.de/en. The measurements were taken at 15-minute intervals, specifically during the time frame of 12:00 pm to 12:15 pm. We refer to 12 pm production as it provides a benchmark for the maximum PV production at this hour. Our analysis is based on 1825 observations for PV production. In this paper, we only cover the area shown in Figure 2.

Figure 2: Transmission system operators in Germany.

Furthermore, Table 1 displays the descriptive statistics. The data presented in the table indicates that the mean production levels at 12 p.m. for 50Hertz, Amprion, and TransnetBW are 3782.77 MW, 3266.2 MW, and 1979.19 MW, respectively. Additionally, it was determined that the dataset demonstrates a right-skewed distribution and negative kurtosis, indicating non-normality.

Table 1: Descriptive data for the operators.

Operators	Min	Max	Mean	Std. Dev.	Skewness	Kurtosis
50Hertz	166	9021	3782.77	2235.38	0.19	-1.10
Amprion	75	7458	3266.20	1789.02	0.17	-1.08
TransnetBW	49	4337	1979.19	1112.62	0.11	-1.23

2.2 Trend and seasonal component

We demonstrate the time series PV power generation of each TSOs in Figure 3. It can be seen that there is an apparent seasonal pattern in the production of each TSOs.

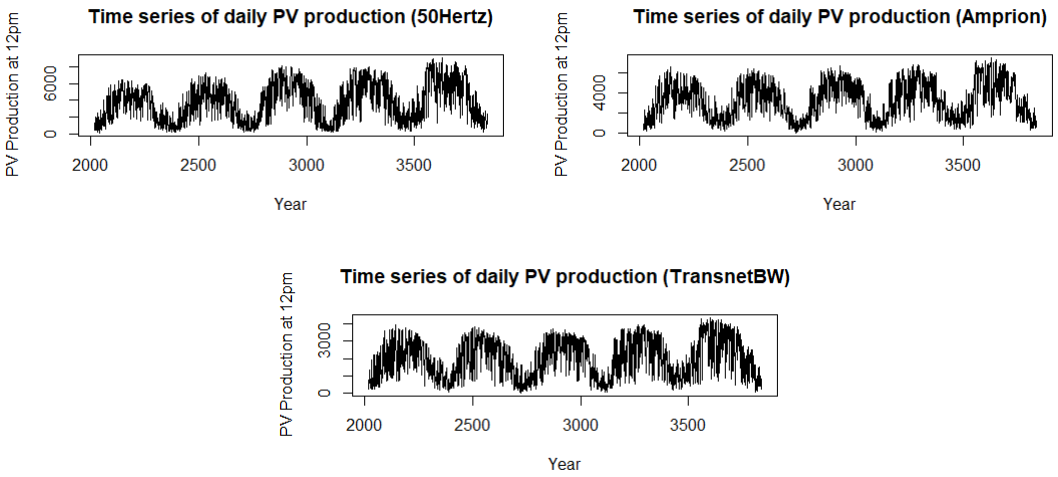

Figure 3: Time series of PV production.

We follow a step-by-step procedure for the data analysis. We first check to see if the trend and seasonality components are present. Next, we employ an autoregressive (AR) model to capture the stochastic behaviour observed in the deseasonalized data. Subsequently, the probabilistic characteristics are determined through the execution of an analysis on the error terms. The time series and the PV production's autocorrelation function (ACF) show strong seasonal effects, as in Figures 3 and 5, respectively. By following the proposed forecasting model by Benth and Ibrahim [5], the PV model is as follows:

$$\ln\big(PV(t)\big) = \Lambda(t) + X(t), \tag{1}$$

where,

$$\Lambda(t) = a + bt + c\ln(I(t)). \tag{2}$$

The suggested model represents a combination of a deterministic, $\Lambda(t)$ and stochastic function, $X(t)$. In this example, we define $PV(t)$ as the PV generation where $t = 0, 1, 2, \ldots, 1825$ days commencing from 12 pm. The variable a denotes the mean level of PV production, while b represents the growth rate resulting from the expansion of capacity. The variable $I(t)$ is used to denote the

intensity of the sun, which is employed to describe its cyclical pattern, with c serving as a scaling parameter. One can refer to the paper of Benth and Ibrahim [5] for a complete sun intensity function. In the following subsection, we will explore an appropriate framework for the stochastic component, $X(t)$.

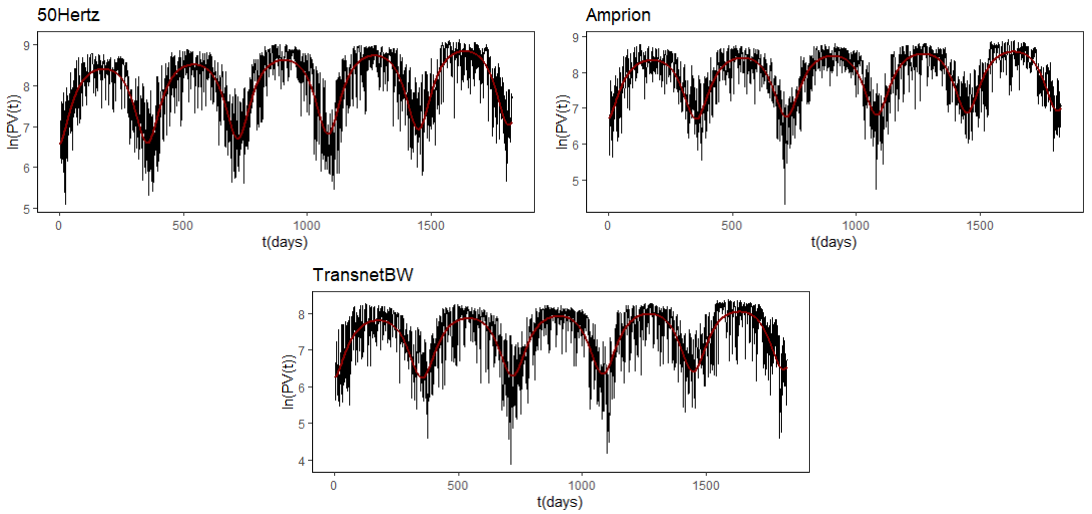

Figure 4: Fitted curve of 12 pm generation (red - ln(I(t)), black - ln(PV (t)).

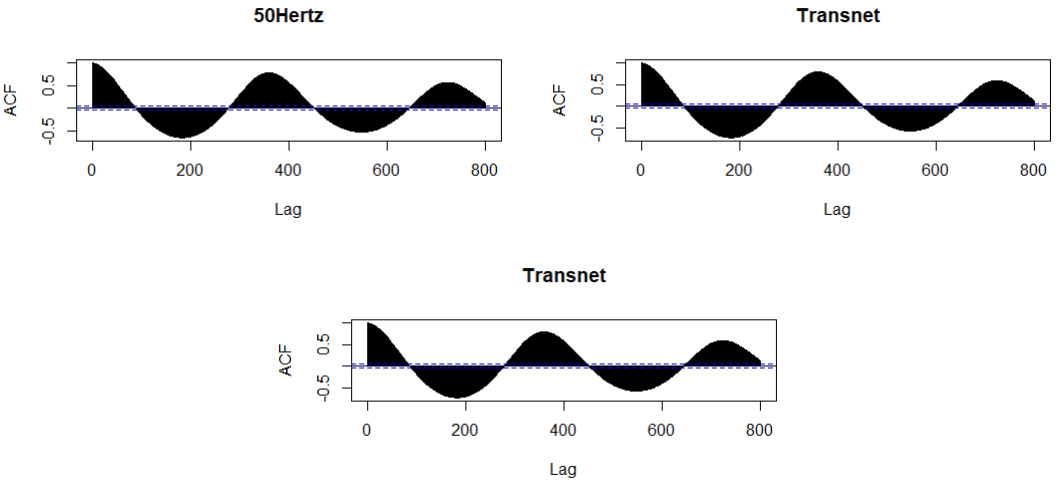

Figure 5: ACF plots.

In temperature variations, we found that to model the seasonality components, few past studies used a cyclical trigonometric function with annual periodicity [7, 9] and Härdle and Cabrera [22] same case as for PV production Ibrahim [24] and Veraart [36]. We consider applying the solar intensity function, which has a clear physical purpose, rather than a summation of trigonometric functions [5]. The sun intensity function, $I(t)$, considers air mass and earth angle to determine how much solar radiation is captured, determining how the solar panels store much sunlight. The variable c in eq. (2) represents the conversion factor that transforms the theoretical maximum

solar energy that may be harnessed into the actual energy production achieved. The solar panel area, cell quality, location, and other factors are taken into consideration by the conversion factor c.

We use lm function in R programming to capture deterministic factors. Table 2 displays the outcomes obtained. Considering that the p values are below the significant level, $\alpha = 0.05$, all parameter estimations are highly significant. The estimated b parameters have positive values, which indicates the upward trend in the mean level of PV production for all TSOs. It is worth noting that the parameters a and c display a reasonable level of stability across all three operators.

Table 2: Measured variables for linear trend and seasonal function.

Operators	$\hat{a}$	$\hat{b}$	$\hat{c}$
50Hertz	8.643435	0.0002995543	3.479342
Amprion	8.606665	0.0001611598	3.422112
TransnetBW	8.083443	0.0001634870	3.864585

As shown in Figure 4, the seasonality behavior of PV production is well captured with the proposed deterministic function, $\Lambda(t)$, represented by the red curve and Figure 5 show their autocorrelation function (ACF). The deseasonalized PV power is calculated by eliminating the linear trend and seasonal components as shown:

$$X(t) = \ln(PV(t)) - \Lambda(t). \tag{3}$$

2.3 An autoregressive model

In Figure 6, we plot the ACF and partial autocorrelation function (PACF) of deseasonalized data. The results demonstrated that the ACF of the deseasonalized data decayed with time, while the PACF cut off at certain lags. These show a signal of the AR process. Since it is difficult to determine the correct order or AR process using the ACF plot, we refer to the PACF plot, demonstrating that the AR process with order one is sufficient to capture the AR structure in the random process of PV generation of 50Hertz and Amprion. However, TransnetBW requires AR process with order two. To simplify the computation, we use the autoregressive process with order two for all operators as in the following function:

$$X(t) = \beta_1 X(t-1) + \beta_2 X(t-2) + \varepsilon(t), \tag{4}$$

where β_1 and β_2 are constants and $\varepsilon(t)$, $t = 1, 2, \ldots$ are the error terms of the AR(2) process that are independent, and identically distributed (i.i.d) random variables.

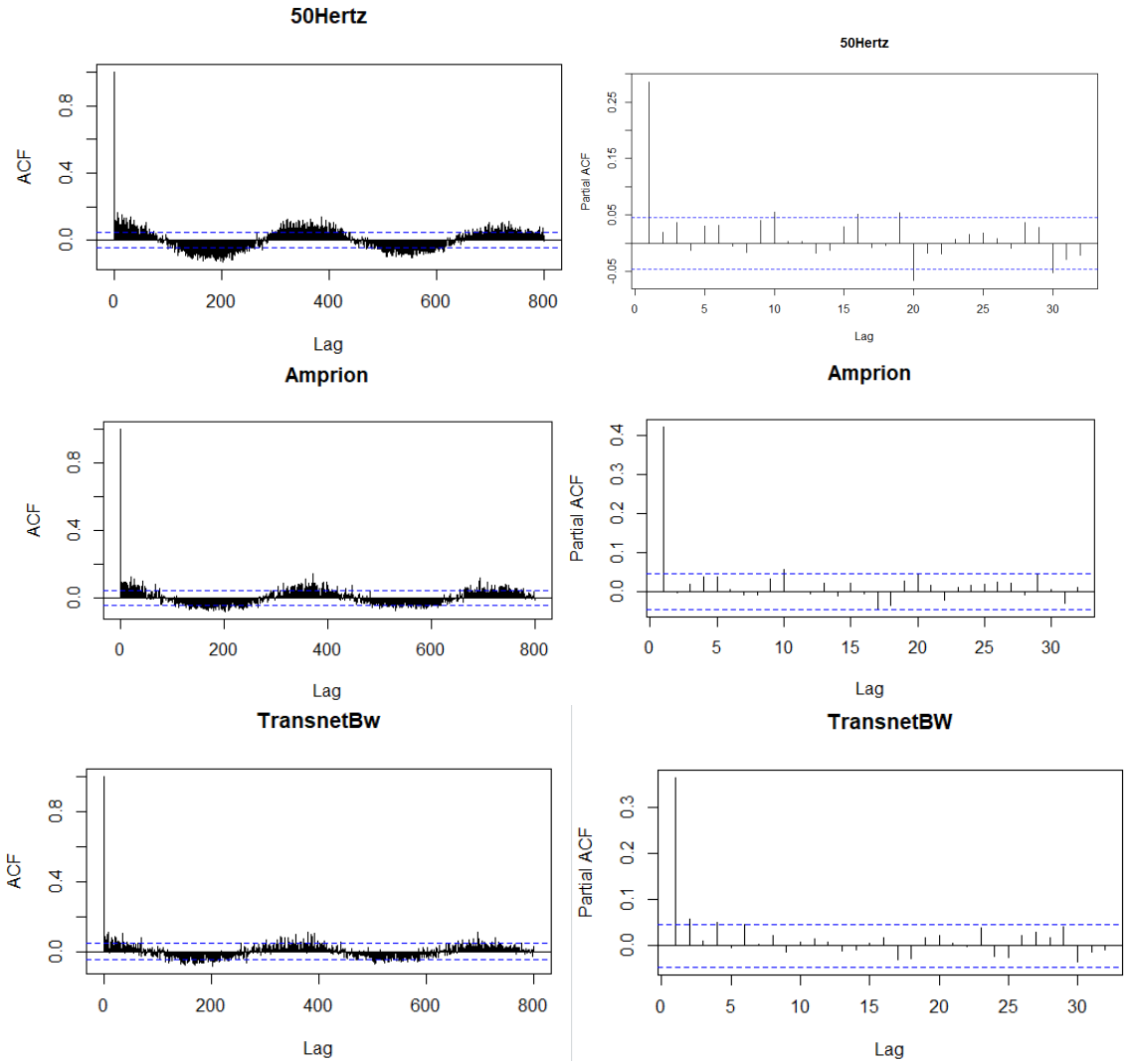

Figure 6: (Left) ACF, (Right) PACF of deseasonalized data.

Table 3 shows the estimated parameters of AR(2). We use R programming to test the AR process's stationarity with the Augmented Dickey-Fuller (ADF) and Kwiatkowski-Phillips-Schmidt-Shin (KPSS) tests. The fitted AR(2) models are stationary because all three moduli of the AR polynomial roots are outside the unit circle.

Table 3: Regression parameter of AR(2) process.

Operators	β_1	β_2
50Hertz	0.2807	0.0194
Amprion	0.4214	-0.0031
TransnetBW	0.3429	0.0585

2.4 Error terms

In this subsection, we proceed with the error terms analysis $\varepsilon(t)$. The graphical representations depicted in Figure 7 provide evident indications of the presence of seasonal heteroskedasticity within the error data. Additionally, it is worth mentioning that the p-values displayed in Table 4 with 5% significant level demonstrate a small magnitude for all TSOs. Furthermore, Figure 8 illustrates a density distribution that exhibits left skewness and a significant leftward tail. These imply that the error terms do not follow normal distribution. The descriptive results is reported in Table 4.

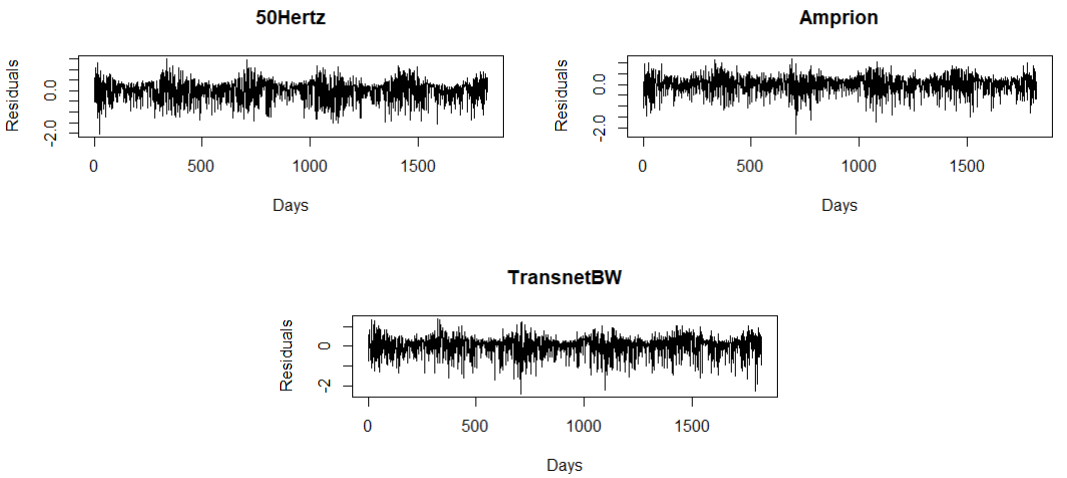

Figure 7: Error Terms.

Table 4: K-S value, p-value, Skewness, Kurtosis (Error Terms).

Operators	K-S statistics	p-value	Skewness	Kurtosis
50Hertz	0.20579	2.476×10^{-7}	-0.55	0.49
Amprion	0.23961	2.476×10^{-7}	-0.75	1.39
TransnetBW	0.21114	2.476×10^{-7}	-0.90	1.28

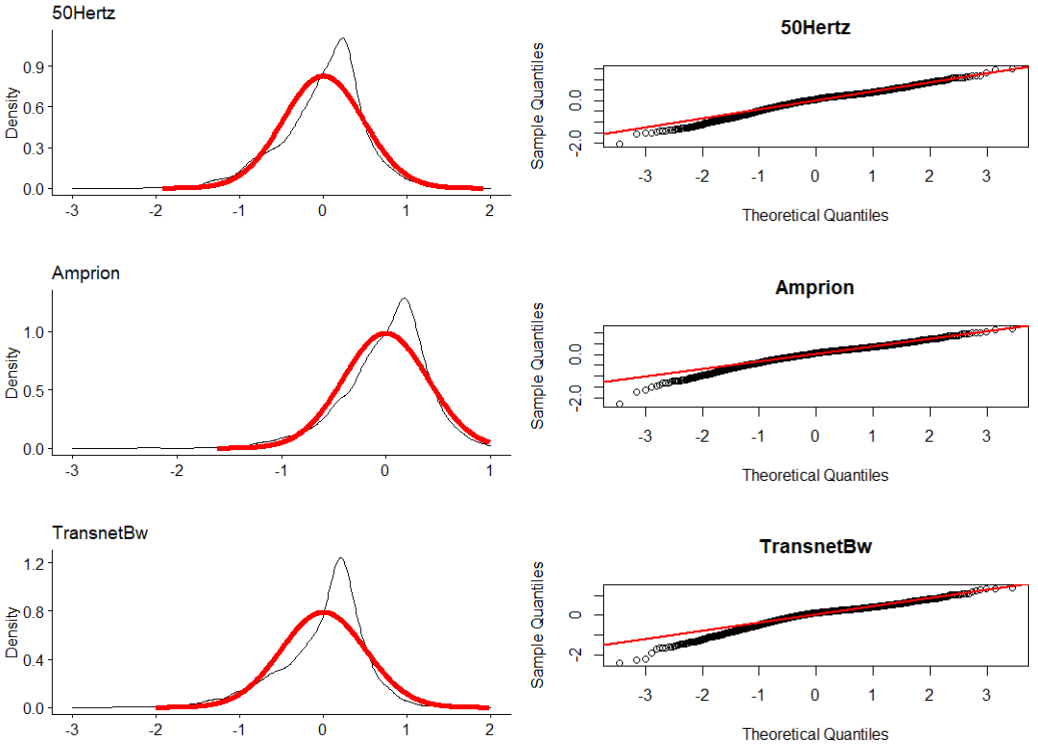

Figure 8: (Left) Density. (Right) Q-Qplot of Error Terms.

We first plot the ACF of the squared error components, as shown in Figure 9, in order to establish a suitable model for the seasonal volatility exhibited in Figure 7. The plots show a clear seasonal pattern. Therefore, we propose adopting the methodology presented in the work of Benth and Ibrahim [5] and Benth and Šaltytė Benth [7] , wherein a truncated Fourier function was employed representing the seasonality of the residuals. Let,

$$\varepsilon(t) = \sigma(t)\bar{\varepsilon}(t), \tag{5}$$

where $\sigma(t)$ represents the square root of a truncated Fourier series, in which

$$\sigma^2(t) = b_1 + \sum_{l=1}^{L} \left(b_{2l} \cos\left(\frac{2l\pi t}{365}\right) + b_{2l+1} \sin\left(\frac{2l\pi t}{365}\right) \right), \tag{6}$$

and $\bar{\varepsilon}(t)$ represent the $standardized$ error terms with $t = 1, 2, \ldots, 1825$.

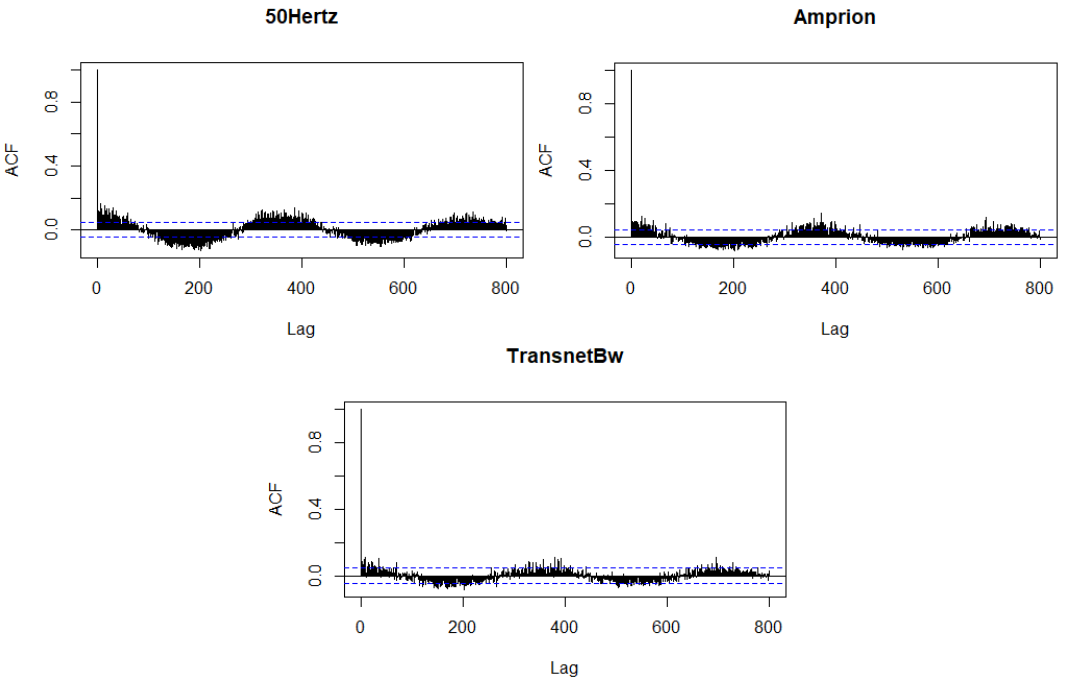

Figure 9: ACF Squared Residual.

In order to execute this procedure, we collect the squared error values correspond to the first week of each year, subsequently calculating their average and assigning them the label "Group 1" (consisting of 28 data points per week, spanning from 2016 to 2020). We repeat the same step until week 52. We then use the nonlinear least squares approach, which uses the nls function in R programming to fit $\sigma^2(t)$ to our data, as approached by Benth and Šaltytė Benth [8]. As a result, the midweek is used as temporal data points within the fitting function of the function $\sigma^2 t$, where t denotes Thursday within the specific week. We set $L = 1$ in the definition of $\sigma^2(t)$ in eq. (6), as the probability of the estimated variables of L greater than one are not significant. We report the results of estimated parameters in Table 5, while the fitted plot in Figure 10 shows that the proposed model may fit the averaged squared error terms well. Based on the plots, we can conclude that winter variations are higher than summer.

Table 5: Fitted parameters of $\sigma^2(t)$.

TSOs	b_1	b_2	b_3
50Hertz	3.9445	-3.4466	-1.7155
Amprion	2.7939	-2.4539	-1.1821
TransnetBW	3.5315	-3.0680	-1.4600

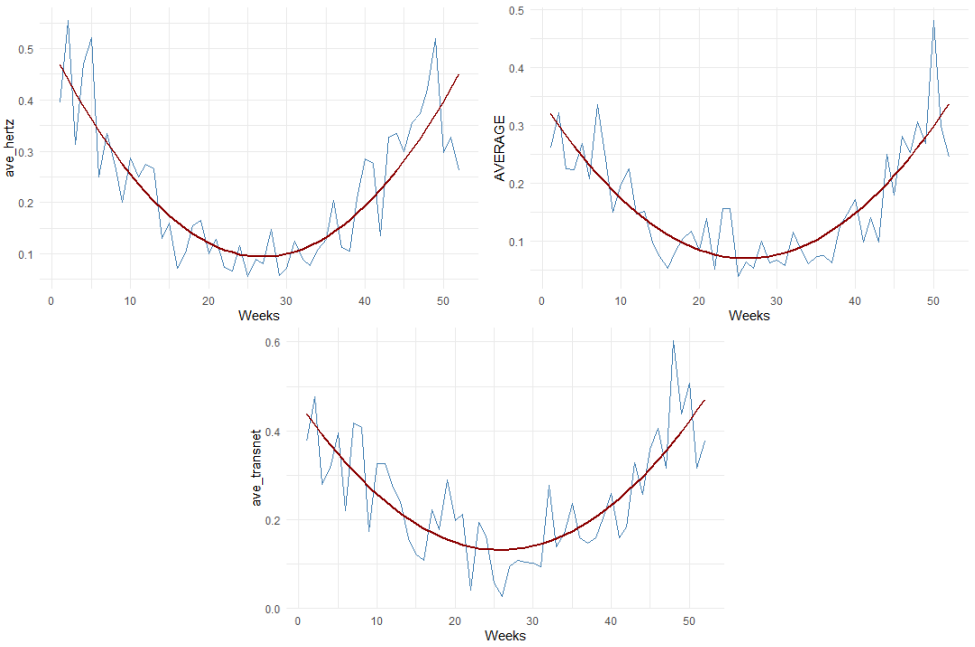

Figure 10: Fitted Average Squared Error Terms.

Figure 11 presents the ACF plots of the standardized and squared standardized error terms. Again, the plots display variation around zero, showing that the proposed model, as in eq. (5), successfully captured the seasonal pattern observed in Figure 9.

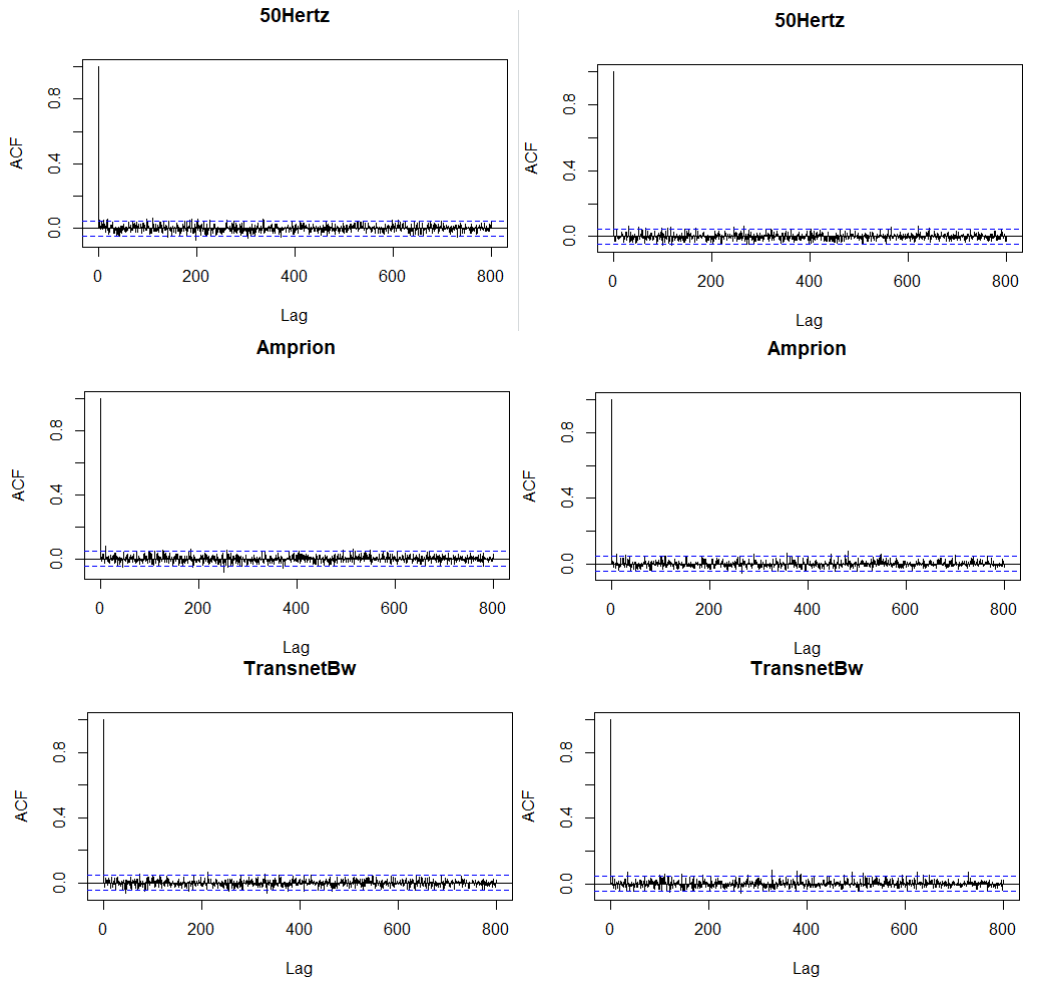

Figure 11: (Left) ACF of Standardized Error Terms, (Right) ACF of Squared Standardized Error Terms.

The density of the standardised error terms in Figure 12 is still abnormal despite the possibility that the proposed model can capture the seasonality behaviour in the error terms. Table 6 presents significant p-values at 5% signifinicant level, while Figure 12 illustrates that the distribution data exhibits negative skewness, as evidenced by the longer tail to the left in the Q-Q plots. The energy market acts in a stylised manner like this. Consequently, the null hypothesis of normality is rejected. The standardized error terms were fit with the skewed normal distribution rather than the normal distribution. The distribution proposed by Azzalini [2] falls within the category of skew-elliptical distributions. This class of distributions is known for its ability to retain the key behaviour of normality, while it also offering additional advantage in accommodating skewness constraints. This method is also used in a few past studies, such as Biagini et al. [10] and Larson et al. [29]. The three parameters for the probability density function are ξ, ω, and α, given by

$$f(x;\xi,\omega,\alpha) = 2\phi(x)\Phi(\alpha x), \tag{7}$$

where ξ, ω and α are location (mean), scale (standard deviation > 0), and shape parameters, correspondingly. On the other hand, $\phi(\cdot)$ indicate the standard normal density and $\Phi(\cdot)$ is its distribution function. In order to include location and scale paramaters, we can transform

$x \to \dfrac{x-\xi}{\omega}$. Thus, the probability density function in eq. (7) becomes

$$f(x) = \frac{2}{\omega}\phi\left(\frac{x-\xi}{\omega}\right)\Phi\left(\alpha\left(\frac{x-\xi}{\omega}\right)\right).$$

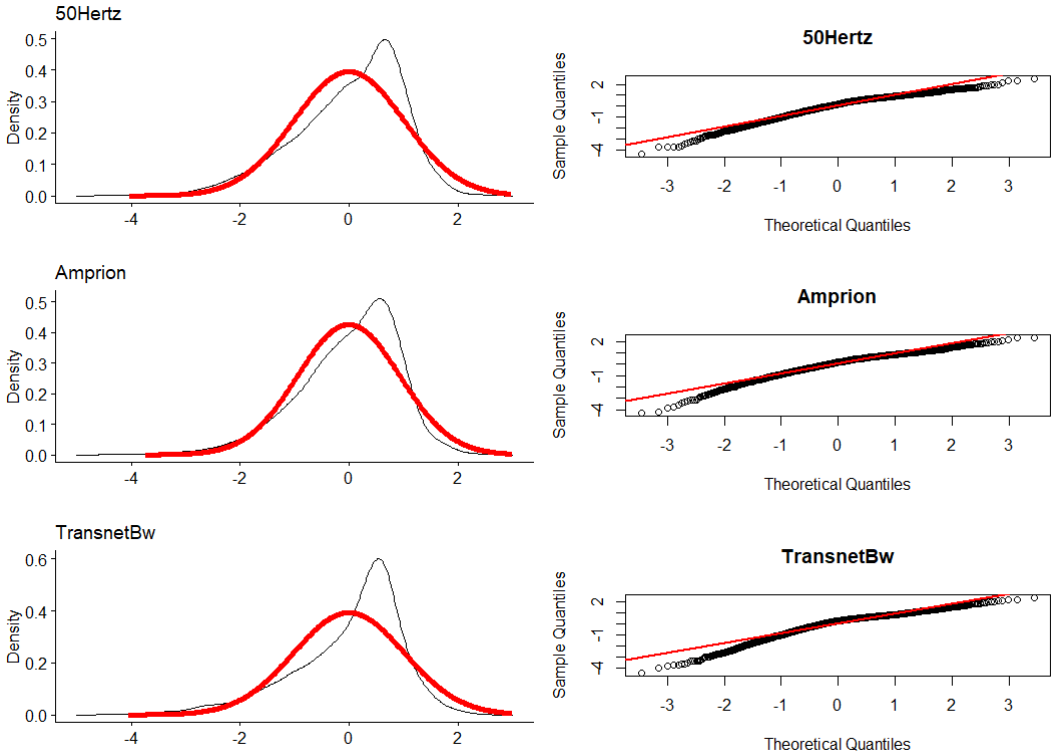

Figure 12: (Left) Density plot. (Right) Q-Q plot of Standardized Error terms.

Table 6: K-S value, p-value, Skewness, Kurtosis (Standardized Error Terms).

Operators	K-S stat	p-value	Skewness	Kurtosis
50Hertz	0.0833	3.344×10^{-5}	-0.82	0.63
Amprion	0.0683	2.716×10^{-3}	-0.86	1.11
TransnetBW	0.1140	2.476×10^{-7}	-1.03	1.16

We fit our standardized error terms with skewed normal distribution using dsn function in R programming. The estimated coefficients and the fitted plots are shown in Table 7 and Figure 13, respectively. Figure 13 shows a reasonably good fit between the fitted skewed normal distribution and the empirical density.

Table 7: Estimated variables of standardized error terms.

Operators	ξ	ω	α
50Hertz	1.193021	1.551259	-3.977338
Amprion	1.068553	1.411560	-3.350651
TransnetBW	1.147100	1.518889	-3.827508

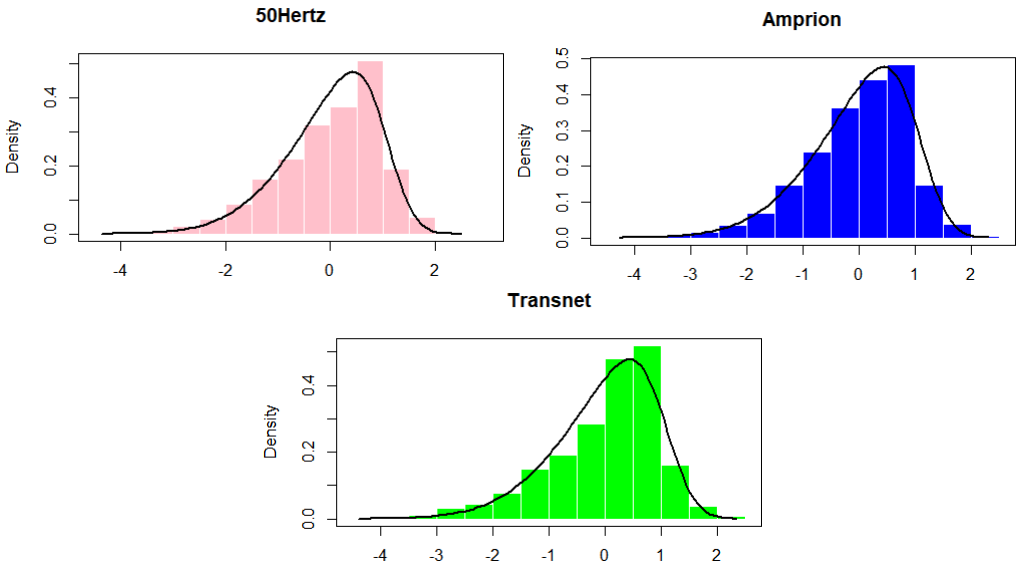

Figure 13: Fitted Skewed Normal Distribution.

2.5 A continuous-time AR(p) dynamics

Due to their mathematical use, we usually choose a continuous-time stochastic process for pricing or hedging a derivative in the mathematical finance field. For instance, Darus and Taib [15] use a continuous time autoregressive moving average (CARMA) to model the temperature insurance pricing. This proves that CARMA process is relevant in energy market. Henceforth, we propose a process in continuous time for the autoregressive models concerning the time series of photovoltaic production and power pricing.

We clarify the stochastic process $\mathbf{Z}(t)$ for $t \in [0, \infty)$ and $p \in \mathbb{N}$ by

$$\mathrm{d}\mathbf{Z}(t) = A\mathbf{Z}(t)\, dt + \mathbf{e}_p \sigma(t)\, dL(t), \tag{8}$$

where A is the $p \times p$-matrix

$$A = \begin{bmatrix} 0 & & I \\ -\alpha_p & \dots & -\alpha_1 \end{bmatrix}, \tag{9}$$

for constants $\alpha_1, \dots, \alpha_p$ are positive values and I is the $(p-1) \times (p-1)$ identity matrix. Therefore, the p'th standard basis vector in $\mathbb{R}^p$ is represented by $\mathbf{e}_p$, and a real-valued square integrable Levy process is represented by L. Given that the σ is measurable and deterministic, with square-integrability over any range of the positive real line, it follows that the function is also integrable

with respect to the Levy process. We have AR(2)-time series model, but along with noise being Gaussian, advocating for the selection of $L = B$, a Brownian motion, and $\sigma(t) = \sigma$. By using system of equations as in Benth and Šaltytė Benth [8], where we transform the AR(2) into CAR(2) process as follows:

$$2 - \alpha_1 = \beta_1,$$
$$\alpha_1 - \alpha_2 - 1 = \beta_2,$$

we presents the fitted regression variable of the CAR(2) model for PV in Table 8.

Table 8: CAR(2)-PVgeneration.

Operators	α_1	α_2
50Hertz	1.7193	0.6999
Amprion	1.5786	0.5817
TransnetBW	1.6571	0.5986

3 Empirical Analysis of Power Prices

3.1 Modelling the electricity spot prices

In this section, we aim to model the electricity spot prices as an application of the proposed PV model. The volume of PV production may impact electricity spot prices. Thus, our main purpose in this section is to discover the relationship between electricity power prices and PV production. For this purpose, we use the same model as proposed by Benth and Ibrahim [5] as follows:

$$S(t) = -\rho \ln PV(t) + R(t). \tag{10}$$

The variable $S(t)$ denotes the spot prices of electricity, with $R(t)$ being the corresponding stochastic process. Additionally, the relationship between energy spot prices and photovoltaic production is depicted by ρ. Since the data on the electricity spot prices are unavailable, we then use the Monte Carlo simulation to get the prices. Noteworthy to mention that we only do the analysis of electricity spot prices for 50Hertz as the results obtained for the other two TSOs are almost similar. Based on the Monte Carlo simulation results, we plot the electricity spot price time series in Figure 14. We observe a clear linear trend in the simulated data. Furthermore, the correlation coefficient is found to be -0.3871. This finding demonstrates the inverse correlation between power spot prices and photovoltaic production.

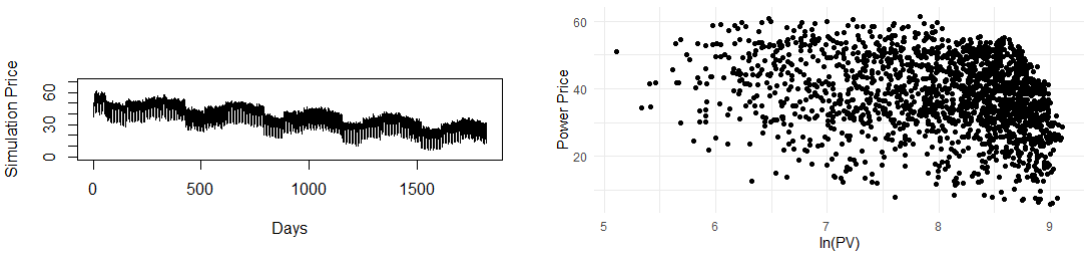

Figure 14: (Left) Time plot series of Power Prices. (Right) Power spot prices vs ln(PV Production).

3.2 Modelling the error term, $R(t)$

Let $R(t)$ represent the combination of the deterministic seasonality function $U(t)$ and the stochastic component $Y(t)$,

$$R(t) = U(t) + Y(t). \tag{11}$$

The notation $U(t)$ present the combination of weekends, seasons, and yearly cyclical patterns where the function is given as follows:

$$U(t) = a + bt + \sum_{i=1}^{2} l_i W_i + \sum_{j=2}^{4} k_j M_j + c\cos\left(\frac{2\pi u(t-v)}{365}\right), \tag{12}$$

where W_i represents the weekend (Saturday and Sunday), while M_j represent the seasonal pattern (winter, summer and fall). To represent weekend and seasonal effects, we use dummy variables, where $W_1 = 1_{t=Saturday}$ and $W_2 = 1_{t=Sunday}$, to represent Saturday and Sunday, respectively. Correspondingly, M_2, M_3 and M_4 represent winter, summer, and fall seasons. We omit one dummy parameter, which is M_1 to avoid perfect multicollinearity. Dummy parameters were used in a number of earlier studies, including Becker et al. [3], Huisman et al. [23] and Ramiah et al. [33] to account for the seasonal trends and deterministic component of electricity costs. The cosine function is used to elaborate the annual cyclical pattern. We use the same estimated coefficient from previous work [5] since we use Monte Carlo simulation to simulate the electrical price based on the electrical price on 31^{st} December 2015. In Table 9, we report the estimated coefficients of $U(t)$. The study reveals that the outcomes during weekends and seasons exhibit a considerable degree of strength, whereas the magnitude of the trigonometric component is merely $c = 1.918$. Plus, estimated coefficients are found to be considerable with $p < 2e-16$ excluded for the final coefficients, u, and v, as the frequency and phase shift, accordingly.

Table 9: Estimated coefficients of seasonality function, $U(t)$.

a	l_1	l_2	k_2	k_3	k_4	b	c	u	v
50.760	-10.340	-18.220	6.380	4.988	7.883	-0.015	1.918	1.069	30.510

We demonstrate the fitted plot, the autocorrelation function (ACF) and partial autocorrelation function (PACF) of the deseasonalized data in Figure 15. It can be observed that we managed to remove the weekend effect shown in Figure 15. The PACF plot shows that AR(3) is sufficient to explain the random factor in the simulated electricity spot prices. We report the estimated coefficient in Table 10. There are no significant lags in the ACF plot of the error terms, as shown in Figure 16. Thus, we can conclude that the error terms are white noise. Furthermore, by observing the density and quantile plots in Figure 17, we may assume that the error terms follow a normal distribution. This has been supported by the insignificant p-value of the K-S statistics, which it found to be 0.092, greater than the significant level, $\alpha = 0.05$. This implies that it is not strong enough to reject the null hypothesis of normality. Based on our analysis, it is recommended to continue utilising Gaussian independent noise for this particular scenario. Upon conducting a meticulous examination of the density and Q-Q plots (refer to Figure 17), it becomes evident that there is a presence of heavy-tailed behaviour. It is worth noting that the residual noise exhibits a good fit with the normal distribution, despite the presence of occasional spikes in the power price data.

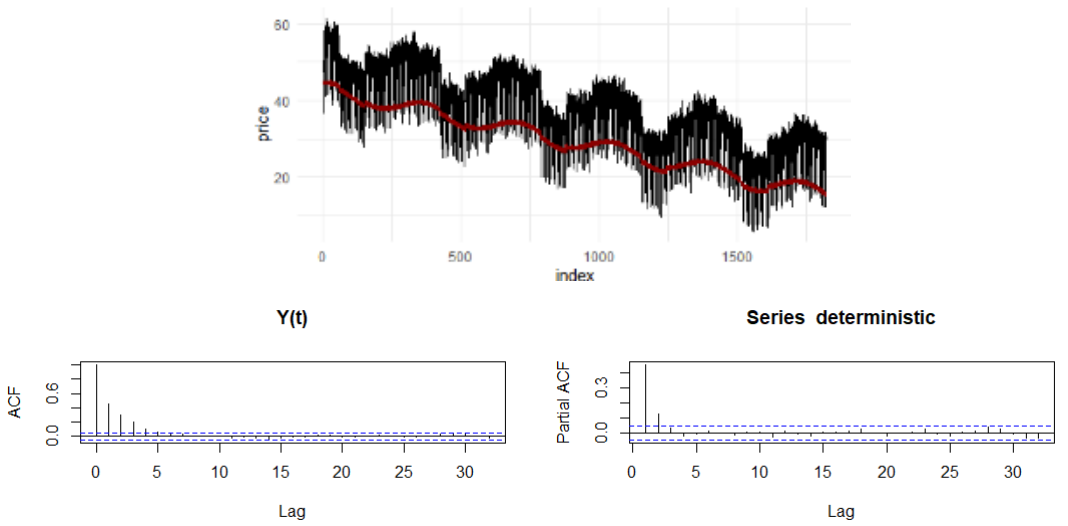

Figure 15: (Above) Fitted curve of power prices. (Bottom Left) ACF of residuals. (Bottom Right) PACF of residuals.

Table 10: Regression parameters of AR(3).

β_1	β_2	β_3
0.404	0.086	0.070

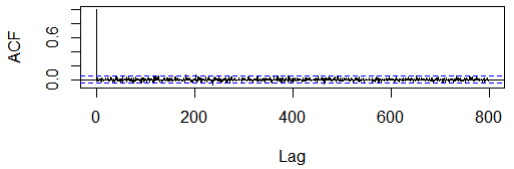

Figure 16: ACF of R(t).

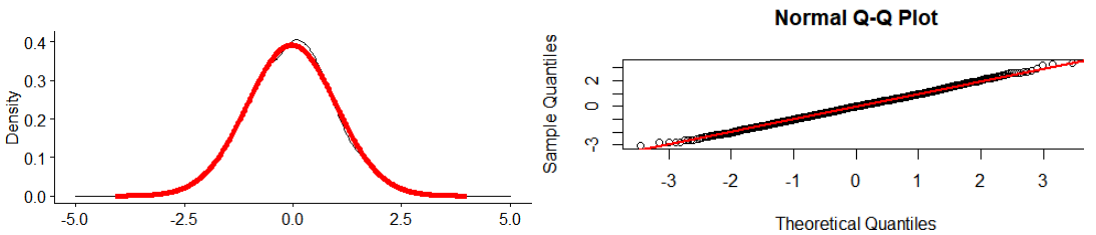

Figure 17: (Left) Plot of error term distribution. (Right) Quantile plot.

We do the same analysis as for power spot price as in Section 2.5. By using system of equations as been used in Benth and Šaltytė Benth [8],

$$3 - \alpha_1 = \beta_1,$$
$$2\alpha_1 - \alpha_2 - 3 = \beta_2,$$
$$\alpha_2 + 1 - (\alpha_1 + \alpha_3) = \beta_3,$$

we display the fitted regression parameters of CAR in Table 11 as follows:

Table 11: Fitted regression coefficients of CAR(3) - Power Spot Price.

α_1	α_2	α_3
2.596	2.107	0.440

4 Quanto Option

Renewable energy has become an important element of the existing energy structure and a main direction of energy development. Wind and solar energy have been developed extensively as typical examples of renewable energy. "Energy" has become the primary use because of the constraints in energy transmission. Overproduction of energy cannot be preserved cost-effectively, and other power sources, such as coal, gas, or nuclear power, must provide for any underproduction. However, power generation from fossil fuels is essential for supply consistency, but they can only satisfy the leftover needs left from renewables, as in the German market. Renewable energy will be hit double due to low PV production and low power prices. We come up with these quanto options to help renewable energy producers. To mitigate the impact of cost and volume risk, it is advisable to explore alternative options that can provide protection against both pricing and supply uncertainties. A put-put mechanism that pertains to the relationship between price and production of photovoltaic energy may be attractive due to its potential benefits.

$$\max\big(L - PV(T), 0\big) \times \max\big(K - S(T), 0\big), \tag{13}$$

the variables K and L are contract-specific, while $S(T)$ and $PV(T)$ represent the power spot price and PV generation, respectively. The notation $\big(L - PV(T)\big) \times \big(K - S(T)\big)$ is the compensation that will be received by the contract's holder in which $PV(T) < L$ (low supply from PV) and $S(T) < K$ (low prices) are situations where the production is at a loss. The preceding discourse pertaining to previous research endeavours, namely Kang et al. [27], Benth et al. [6], Brik and Roncoroni [25], serves as a case study of an energy quanto option. Thus, it is imperative to develop a hybrid model that incorporates both power prices and photovoltaic (PV) production in order to comprehensively analyse the distribution of payoffs, pricing of options, and optimal strike design.

Quanto options have been increasingly popular in the energy markets in recent years. The payoff from such options is usually calculated using an underlying energy index and a temperature measurement. They consider the high correlation between energy usage and particular weather conditions, allowing price and weather risk to be managed together. As a result, these products are more effective and, in many circumstances, less expensive than plain vanilla alternatives [12]. Typically, the available alternatives are determined by a mean pricing value and a meteorological factor, namely a temperature indicator that reflects the level of demand. Power price options are available in several power markets, and the Chicago Mercantile Exchange provides weather-variable derivatives to some extent. On the other hand, Benth et al. [6] describe a method for pricing options that include a pricing measure. Brik and Roncoroni [25] examine the optimum design for such options. Kang and Zhou [28] design an empirical hedging model for energy quanto contracts and explore a few intriguing hedging challenges linked to financial instruments.

Consider an empirical example of a quanto option payoff, as shown in eq. (13). We undertake a Monte Carlo analysis of the payoff histogram and the expected payoff value based on the models for PV production and electricity price derived in the prior sections. Over a year, we have focused on four different quanto option contracts. All four contracts mature in $T = 30$ days from "present," where "present" is (i) 1^{st} January, (ii) 1^{st} April, (iii) 1^{st} July, and (iv) 1^{st} October, with 2021 as the basis year. We perform Monte Carlo simulations of the dynamics of $PV(t)$ and $S(t)$ with $t = 0, 1, 2, \ldots, 30$, presuming $PV(t)$ as a skewed- normal noise and $S(t)$ as a normal noise. The initial values are $X(0) = 0$, so that $PV(0) = \exp(\Lambda(30))$, with $\Lambda(0)$ as the seasonality function at "present" in the four different cases. Next, we let $Y(0) = 0$, so that $S(0) = -\rho \ln PV(0) + U(0)$. As strike prices, we set $L = \exp(\Lambda(30))$ and $K = -\rho(30) + U(30)$. The seasonal values of the PV and spot price at exercise time $T = 30$, ranging by the four seasons, namely winter, spring, summer, and autumn, are conventionally represented by the months of January, April, July, and October, respectively. As a result, at the exercise time, we examine quanto options that would protect PV production exceeding seasonality and spot prices falling below the "seasonal mean".

From 400,000 outcomes in the Monte Carlo simulation, we plotted all four histograms of the payoff functions $\big(\max(L(30) - PV, 0)$ and $\max(K - S(30))\big)$, respectively, in Figures 18 and 19. The PV payoffs vary greatly depending on the season, as in Figure 18. We have low PV production and significant volatility in the winter (January), whereas we have the highest average production and moderate volatility in the summer (July). This is reflected in the histograms in Figure 18, where spring (April) and autumn (October) have the highest spread in the simulated payoffs. The highest frequency of PV production distribution per hour in January is between 0 to 50 MWH, approximately 8000; in April, July, and October, the highest frequency is between 0 to 100MWH, approximately 6000, 7000, and 9000, respectively.

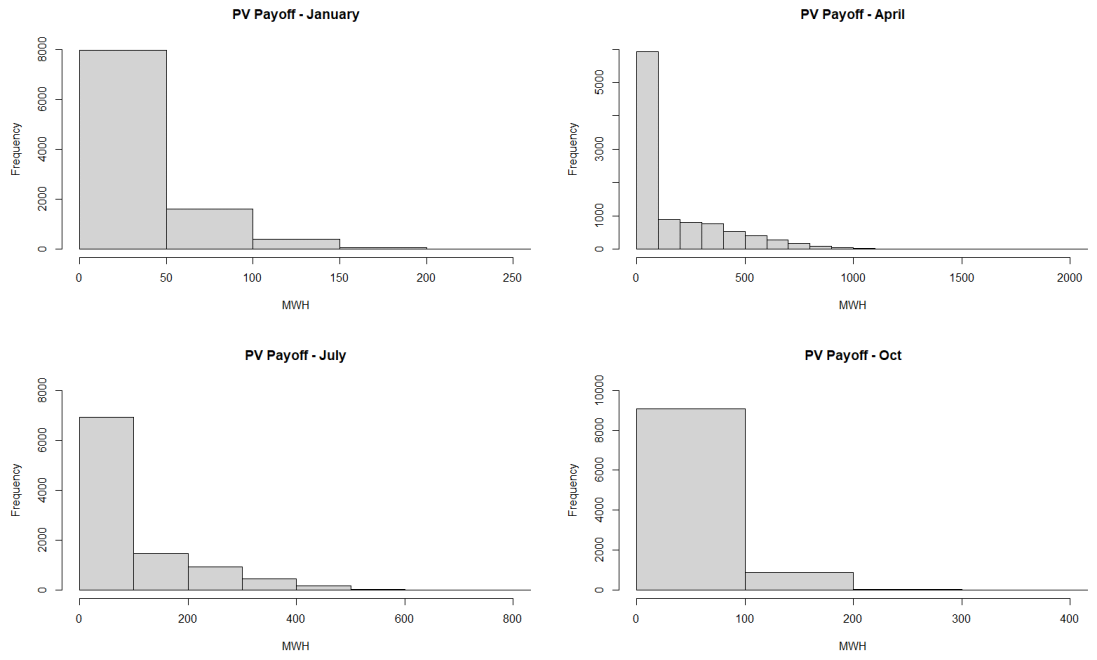

Figure 18: Histogram of payoff function from PV production put option.

Meanwhile, based on Figure 19, the electricity price payoffs are consistent throughout the year. The highest frequency of power prices distribution for January, April, July, and October is between

0 to 1 €/MWH, approximately 7500, 6500, 7000, and 9000, respectively.

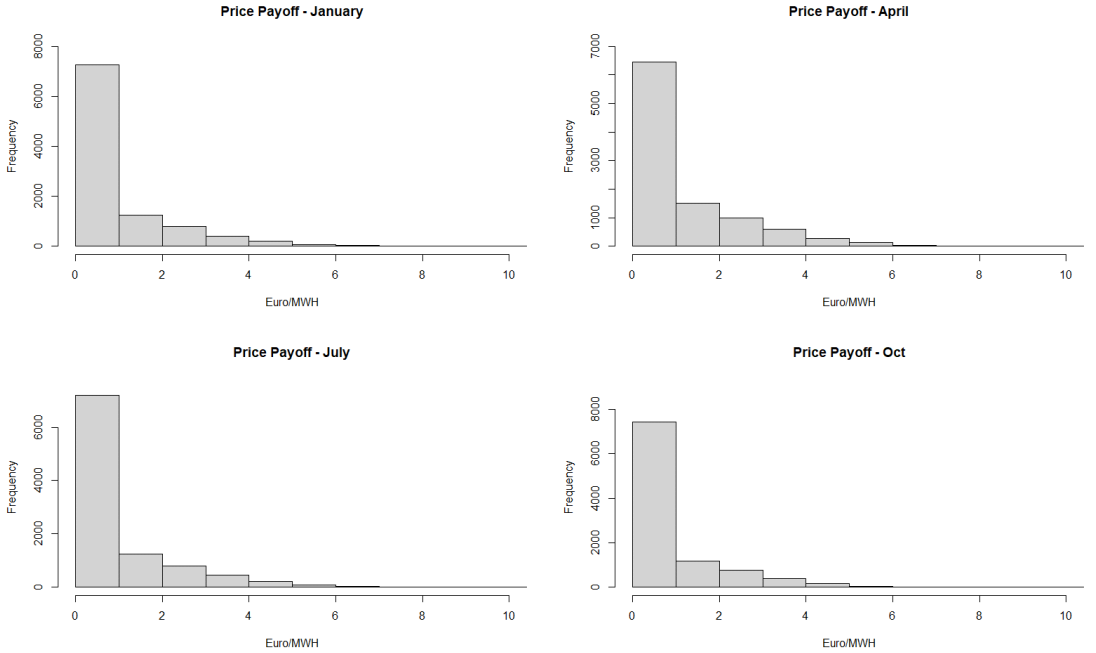

Figure 19: Histogram of payoff function from power price put option.

The payoff of the quanto option for each of the four seasons is shown in Figure 20, where we observed that the highest frequency in January, April, July, and October is between €0 to €100, which amounted to 9500, 8000, 8500 and 8000 respectively. In addition, we can see that the pattern of quanto options payoff of four seasons varies depending on the season, as in the PV payoff in Figure 18.

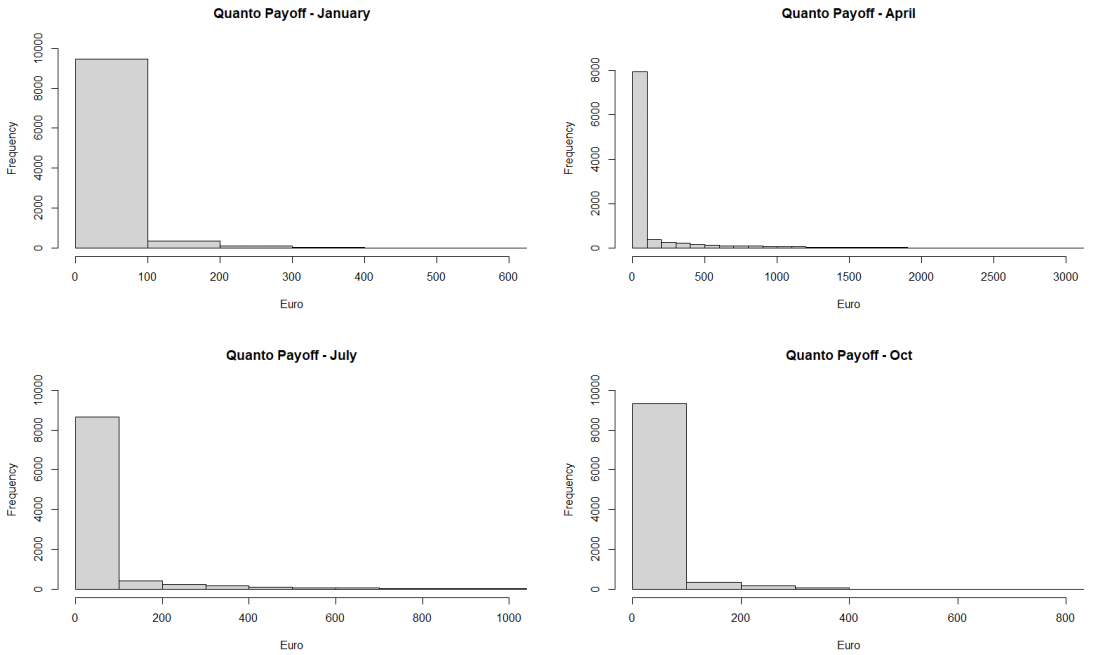

Figure 20: Histogram of payoff function from quanto option.

Next, we compute the quanto options price as in eq. (14), where r is the interest rate. Finally, in Figure 21, we display the histogram of monthly quanto options prices representing each season. For example, the average quanto options price for January is €472.22, April is €3104.40, July is €1160.88 and October is €638.17. The price of the quanto options varies more in July than in other seasons.

$$\sum_{t=0}^{T} e^{-rt}\Big[\max\big(L - PV(T), 0\big) \times \max\big(K - S(T), 0\big)\Big]. \tag{14}$$

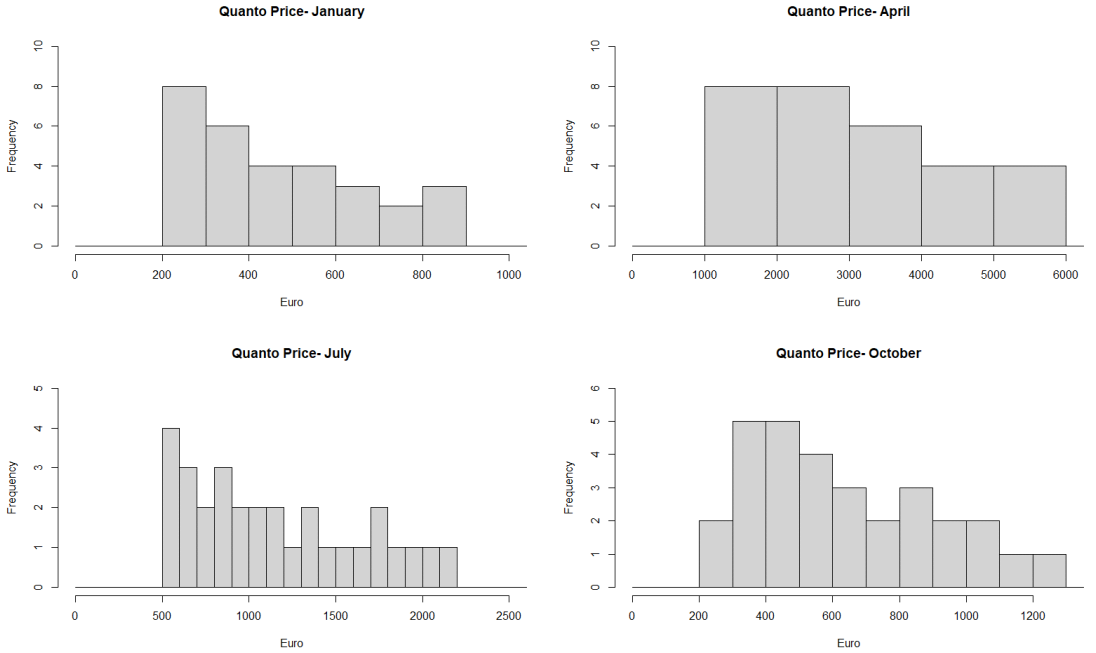

Figure 21: Histogram of quanto price of each month.

5 Conclusion

We have revised the results from earlier work of PV production dynamics employing the intensity of sun to explain the seasonal mean fluctuation. The five years of daily output data at 12 o'clock from three TSOs in Germany served as the basis for our research. The deseasonalized PV production data neatly exhibits a second-order AR process with seasonal volatility and non-Gaussian noise. As a consequence, we recommended simulating the error with the skewed normal distribution.

We looked into a few benefits that our PV model might provide. Initially, we employed PV generation as an independent parameter to analysis dynamics of power price, specifically to establish a correlation between spot prices of electricity and the logarithmic PV production. As a purpose to simulate the cost of electricity, Monte Carlo simulation has been used. After PV generation has been eliminated, the dynamics of the power spot price can be adequately represented by using a simple third-order AR dynamic with normally distributed noise.

Additionally, we deliberated on the potential application of our methodology to analyse contracts related to photovoltaic virtual power plants and quanto options. Our research demonstrates the viability of developing continuous-time models, such as continuous-time autoregressive processes. These methods are beneficial for assessing quanto options, calculating the cost and production risk jointly, and hedging such options. In our case, we concentrate on companies that produce renewable energy. This approach could potentially yield advantages for producers of non-renewable energy sources. Given the significant supply and price risks that both parties are subject to, many novel option structures may be useful for hedging.

We want to find out the quanto option pricing in next study by including the risk-free interest rate as a discount factor. In addition, we aim to model the Levy process for Quanto options since our PV and power prices are not normally distributed. Finally, it would also be interesting to construct models that include wind power generation. These intriguing subjects are left for future discovery.

Acknowledgement This research was supported by Malaysian Ministry of Higher Education under Fundamental Research Grant Scheme (FRGS/1/2020/STG/USIM/02/1).

Conflicts of Interest The authors declare no conflict of interest.

References

[1] M. P. Almeida, O. Perpiñán & L. Narvarte (2015). PV power forecast using a nonparametric PV model. *Solar Energy*, *115*, 354–368. https://doi.org/10.1016/j.solener.2015.03.006.

[2] A. Azzalini (1985). A class of distributions which includes the normal ones. *Scandinavian Journal of Statistics*, *12*(2), 171 – 178. https://www.jstor.org/stable/4615982.

[3] R. Becker, S. Hurn & V. Pavlov (2007). Modelling spikes in electricity prices. *Economic Record*, *83*(263), 371 – 382. https://doi.org/10.1111/j.1475-4932.2007.00427.x.

[4] F. E. Benth, L. Di Persio & S. Lavagnini (2018). Stochastic modeling of wind derivatives in energy markets. *Risks*, *6*(2), Article ID: 56. https://doi.org/10.3390/risks6020056.

[5] F. E. Benth & N. A. Ibrahim (2017). Stochastic modeling of photovoltaic power generation and electricity prices. *Journal of Energy Markets*, *10*(3), 1–33. http://doi.org/10.21314/JEM.2017.164.

[6] F. E. Benth, N. Lange & T. A. Myklebust (2015). Pricing and hedging quanto options in energy markets. *Journal of Energy Markets*, *8*(1), 1–35. http://doi.org/10.21314/JEM.2015.130.

[7] F. E. Benth & J. Šaltytė Benth (2011). Weather derivatives and stochastic modelling of temperature. *International Journal of Stochastic Analysis*, *2011*, Article ID: 576791. https://doi.org/10.1155/2011/576791.

[8] F. E. Benth & J. Šaltytė Benth (2012). *Modeling and Pricing in Financial Markets for Weather Derivatives* volume 17. World Scientific, London, UK.

[9] F. E. Benth & C. M. I. C. Taib (2013). On the speed towards the mean for continuous time autoregressive moving average processes with applications to energy markets. *Energy Economics*, *40*, 259 – 268. https://doi.org/10.1016/j.eneco.2013.07.007.

[10] F. Biagini, J. Bregman & T. Meyer-Brandis (2015). Electricity futures price modeling with levy term structure models. *International Journal of Theoretical and Applied Finance*, *18*(1), Article ID: 1550003. https://doi.org/10.1142/S021902491550003X.

[11] S. Borovkova & M. D. Schmeck (2017). Electricity price modeling with stochastic time change. *Energy Economics*, *63*, 51 – 65. https://doi.org/10.1016/j.eneco.2017.01.002.

[12] M. Caporin, J. Preś & H. Torro (2012). Model based Monte Carlo pricing of energy and temperature Quanto options. *Energy Economics*, *34*(5), 1700 – 1712. https://doi.org/10.1016/j.eneco.2012.02.008.

[13] M. S. Chowdhury, K. S. Rahman, T. Chowdhury, N. Nuthammachot, K. Techato, M. Akhtaruzzaman, S. K. Tiong, K. Sopian & N. Amin (2020). An overview of solar photovoltaic panels end-of-life material recycling. *Energy Strategy Reviews*, *27*, Article ID: 100431. https://doi.org/10.1016/j.esr.2019.100431.

[14] K. Cui & A. V. Swishchuk (2015). Applications of weather derivatives in the energy market. *Journal of Energy Markets*, *8*(1), 1 – 18. http://doi.org/10.21314/JEM.2015.132.

[15] M. Darus & C. M. I. C. Taib (2022). Modelling temperature using CARMA processes with Stochastic speed of mean reversion for temperature insurance pricing. *Malaysian Journal of Mathematical Sciences*, *16*(2), 273 – 288. https://doi.org/10.47836/mjms.16.2.07.

[16] X. Deng, P. Zhang, K. Jin, J. He, X. Wang & Y. Wang (2019). Probabilistic load flow method considering large-scale wind power integration. *Journal of Modern Power Systems and Clean Energy*, *7*(4), 813 – 825. https://doi.org/10.1007/s40565-019-0502-0.

[17] A. Dolara, F. Grimaccia, S. Leva, M. Mussetta & E. Ogliari (2015). A physical hybrid artificial neural network for short term forecasting of PV plant power output. *Energies*, *8*(2), 1138 – 1153. https://doi.org/10.3390/en8021138.

[18] G. Dutta & K. Mitra (2017). A literature review on dynamic pricing of electricity. *Journal of the Operational Research Society*, *68*(10), 1131–1145. https://doi.org/10.1057/s41274-016-0149-4.

[19] EIA. Energy and the environment explained: Where greenhouse gases come from. Technical report U.S. Energy Information Administration Washington 2020. https://www.eia.gov/energyexplained/energy-and-the-environment/where-greenhouse-gases-come-from.php.

[20] J. Esunge & J. J. Njong (2020). Weather derivatives and the market price of risk. *Journal of Stochastic Analysis*, *1*(3), Article ID: 7. https://doi.org/10.31390/josa.1.3.07.

[21] D. Gielen, F. Boshell, D. Saygin, M. D. Bazilian, N. Wagner & R. Gorini (2019). The role of renewable energy in the global energy transformation. *Energy Strategy Reviews*, *24*, 38 – 50. https://doi.org/10.1016/j.esr.2019.01.006.

[22] W. K. Härdle & B. L. Cabrera (2012). The implied market price of weather risk. *Applied Mathematical Finance*, *19*(1), 59 – 95. https://doi.org/10.1080/1350486X.2011.591170.

[23] R. Huisman, C. Huurman & R. Mahieu (2007). Hourly electricity prices in day-ahead markets. *Energy Economics*, *29*(2), 240–248. https://doi.org/10.1016/j.eneco.2006.08.005.

[24] N. A. Ibrahim (2021). Modelling of intraday Photovoltaic power production. *Malaysian Journal of Science*, *40*(2), 105 – 124. https://doi.org/10.22452/mjs.vol40no2.8.

[25] R. Id Brik & A. Roncoroni (2016). Static mitigation of volumetric risk. *Journal of Energy Markets*, *9*(2), 111 – 150. https://doi.org/10.21314/JEM.2016.146.

[26] IRENA (2019). *Global Energy Transformation: A Roadmap to 2050*. International Renewable Energy Agency, Abu Dhabi 2019 edition. https://www.irena.org/publications/2019/Apr/Global-energy-transformation-A-roadmap-to-2050-2019Edition.

[27] S. B. Kang, M. Ong & J. Zhao (2019). A new approach to evaluating the cost-efficiency of complex hedging strategies: an application to electricity price volume quanto contracts. *Journal of Energy Markets*, *12*(3), 1 – 27. http://doi.org/10.21314/JEM.2018.187.

[28] S. B. Kang & J. Zhao (2017). An analytic hedging model of energy quanto contracts. *Theoretical Economics Letters*, *7*(4), 737 – 746. https://doi.org/10.4236/tel.2017.74053.

[29] D. P. Larson, L. Nonnenmacher & C. F. M. Coimbra (2016). Day-ahead forecasting of solar power output from photovoltaic plants in the American Southwest. *Renewable Energy*, *91*, 11 – 20. https://doi.org/10.1016/j.renene.2016.01.039.

[30] Y. Lee, H. Yoo & J. Lee (2017). Pricing formula for power quanto options with each type of payoffs at maturity. *Global Journal of Pure and Applied Mathematics*, *13*(9), 6695 – 6702. https://www.ripublication.com/gjpam17/gjpamv13n9_174.

[31] A. Mohamed & B. Chowdhury (2016). Solar power forecasting using support vector regression. In *International Annual Conference of the American Society for Engineering Management 2016* (*ASEM 2016*), pp. 6 pages. American Society for Engineering Management, North Carolina, USA.

[32] S. Prakash, N. P. Gopinath & J. Suganthi (2017). Wind and solar energy forecasting system using artificial neural networks. *International Journal of Pure and Applied Mathematics*, *118*(5), 845 – 854.

[33] V. Ramiah, S. Thomas, R. Heaney & H. Mitchell (2015). *Seasonal Aspects of Australian Electricity Market*, pp. 935 –956. Springer New York, New York. https://doi.org/10.1007/978-1-4614-7750-1_33.

[34] B. Taştan & A. Hayfavi (2017). Modeling Temperature and Pricing Weather Derivatives Based on Temperature. *Advances in Meteorology*, *2017*, Article ID: 3913817. https://doi.org/10.1155/2017/3913817.

[35] L. Teng, M. Ehrhardt & M. Günther (2015). The pricing of Quanto options under dynamic correlation. *Journal of Computational and Applied Mathematics*, *275*, 304 – 310. https://doi.org/10.1016/j.cam.2014.07.017.

[36] A. E. D. Veraart (2016). Modelling the impact of wind power production on electricity prices by regime-switching Lévy semistationary processes. In F. E. Benth & G. Di Nunno (Eds.), *Stochastic of Environmental and Financial Economics*, pp. 321 – 340. Springer International Publishing, Cham. https://doi.org/10.1007/978-3-319-23425-0_13.

[37] Z. Wang, P. Li, L. Li, C. Huang & M. Liu (2015). Modeling and Forecasting Average Temperature for Weather Derivative Pricing. *Advances in Meteorology*, *2015*, Article ID: 837293. https://doi.org/10.1155/2015/837293.

[38] B. Wolff, J. Kühnert, E. Lorenz, O. Kramer & D. Heinemann (2016). Comparing support vector regression for PV power forecasting to a physical modeling approach using measurement, numerical weather prediction, and cloud motion data. *Solar Energy*, *135*, 197 – 208. https://doi.org/10.1016/j.solener.2016.05.051.

[39] H. Zhu, W. Lian, L. Lu, S. Dai & Y. Hu (2017). An improved forecasting method for photovoltaic power based on adaptive BP neural network with a scrolling time window. *Energies*, *10*(10), Article ID: 1542. https://doi.org/10.3390/en10101542.